AIP | The Journal of Chemical Physics

Vibrational and structural properties of amorphous n-butanol: A complementary Raman spectroscopy and X-ray diffraction study

Alain Hédoux, Yannick Guinet, L. Paccou, P. Derollez, and F. Danède

Citation: The Journal of Chemical Physics **138**, 214506 (2013); doi: 10.1063/1.4808159
View online: http://dx.doi.org/10.1063/1.4808159
View Table of Contents: http://scitation.aip.org/content/aip/journal/jcp/138/21?ver=pdfcov
Published by the AIP Publishing

Vibrational and structural properties of amorphous n-butanol: A complementary Raman spectroscopy and X-ray diffraction study

Alain Hédoux,[a] Yannick Guinet, L. Paccou, P. Derollez, and F. Danède
UMET UMR CNRS 8207, Université Lille Nord de France, F-59000 Lille, France and USTL, F-59655 Villeneuve d'Ascq, France

(Received 13 March 2013; accepted 16 May 2013; published online 7 June 2013)

Raman spectroscopy and X-ray diffraction experiments were performed in the liquid, undercooled liquid, and glassy states of n-butanol. Clear correlated signatures are obtained below the melting temperature, from both temperature dependences of the low-wavenumber vibrational excitations and the intermediate-range order characterized by a prepeak detected in the different amorphous states. It was found that these features are related to molecular associations via strong hydrogen bonds, which preferentially develop at low temperature, and which are not compatible with the long-range order of the crystal. This study provides information on structural heterogeneities developing in hydrogen-bonded liquids, associated to the undercooled regime and the inherent glass transition. The analysis of the isothermal abortive crystallization, 2 K above the glass transition temperature, has given the opportunity to analyze the early stages of the crystallization and to describe the origin of the frustration responsible for an uncompleted crystallization. © *2013 AIP Publishing LLC*. [http://dx.doi.org/10.1063/1.4808159]

I. INTRODUCTION

Many molecular liquids can be easily supercooled, leading to the vitrification of the material accompanied by the intense and intriguing slowing down of the molecular dynamics approaching the glass transition temperature in fragile systems.[1] However, structural properties and signatures associated with this metastable situation and the vitrification mechanism, remain elusive. Polyamorphic transitions and the related mechanisms of the glass transition have recently focused great attention from the evidence of a first-order transition between the supercooled liquid and an apparently amorphous state, named glacial state, in triphenyl phosphite (TPP)[2,3] and n-butanol.[4,5] Such a transition was considered as a first-order liquid-liquid phase transition.[5] On the other hand, the glacial state was considered as the signature of defect-ordered phase, characterized by a crystalline symmetry incompatible with space tiling,[2] and corresponding to the existence of a preferred local structure developing in the deeply undercooled liquid.[6] From Raman, X-ray diffraction, and thermodynamic investigations on TPP[7–9] and n-butanol,[10–12] the apparently second amorphous state was described as a nano-/micro-crystalline state resulting from an abortive crystallization process. A detailed structural analysis of glacial and crystalline TPP[9,13] has shown that the glacial state could be interpreted as a heavily nucleated state composed of micro- or nano-crystals of the stable crystalline phase. The frustration responsible for the abortive crystallization was attributed to a very high nucleation rate in a temperature range where the growth rate is low.[7]

n-butanol is an associated liquid, as other alcohols, characterized by their great ability to form molecular associations through intermolecular H-bonds, corresponding to heterogeneities of a few nanometers. It was suggested, from Raman investigations, that the origin of the frustration responsible for the abortive crystallization of n-butanol was related to rearrangement of H-bonded molecules.[10] The existence of linear chains of about ten molecules in the liquid state of several alcohols was shown via the analysis of the prepeak, which is considered as the signature of correlations between hydrogen-bonded alcohol molecules.[14] The connection between these molecular associations and structural heterogeneities suspected to be involved in the slowing-down of the dynamics approaching the glass transition[6,15] is still unclear. Raman spectroscopy investigations[10] have revealed the existence of different kinds of intermolecular associations in the amorphous (liquid and glass) and crystalline (glacial and crystal) states. The present study reports on the analysis of these different H-bond networks, developing in the amorphous (glass, supercooled liquid, and liquid), glacial, and crystalline states in relation with structural properties to get a better insight on the origin of the glacial state and on the relation between intermolecular associations and the glass transition mechanism. Raman spectroscopy was used to analyze the H-bond networks in the intramolecular O–H stretching region and their correlation on the low-frequency excitations. The structural signatures of the H-bond networks were analyzed from X-ray diffraction experiments. These investigations were interpreted on the basis of recent diffraction studies[11,16] in crystalline and glacial n-butanol, to give a more detailed description of the H-bond networks in the different states of n-butanol and to better determine their involvement in the mechanisms of frustrated crystallization and glass transition.

[a]Author to whom correspondence should be addressed. Electronic mail: alain.hedoux@univ-lille1.fr

II. EXPERIMENTAL

A. Material

n-butanol was purchased at 99% purity from Aldrich and used without further purification. The sample was first heated from room temperature up to 400 K at 6 K/min. The sample was then analyzed upon cooling by steps of 20 K from 400 K down to 180 K, and then by steps of 10 K down to 90 K. An Oxford open gas-flow cryostat that keeps temperature fluctuations within ±0.1 K was used for X-ray and Raman investigations. Counting time for each diffraction pattern was 30 min for X-ray diffraction, and 10 min for Raman spectroscopy. The sample was heated up to 120 K (2 K above T_g) for isothermal annealing. Counting time was 10 min for analyzing the isothermal transformation of the supercooled liquid in the glacial state both by X-ray diffraction and Raman spectroscopy. After 8 h, the undercooled liquid was isothermally transformed into the glacial state. After transformation, the sample was further heated at 165 K (6 K/min) for obtaining the overall crystallization, and then cooled down to 110 K only for analyzing the crystalline state by Raman spectroscopy.

B. Methods

1. X-ray diffraction

Data acquisition of the x-ray diffraction patterns in the different states of n-butanol was performed with an Inel curved position-sensitive gaseous detector (CPS 120). This detector consists of 4096 channels with an angular step approximately equal to 0.015 that cover a range of 120° 2θ. The vertical Debye-Scherrer geometry, operating with a monochromatic Cu Kα_1 radiation ($\lambda = 1.54056$ Å) selected with an incident-beam curved-quartz monochromator, was used. The diffractometer was computer controlled using the Symphonix software (Inel) and was calibrated using the attenuated direct beam at 2° intervals. The minimum instrumental full width at half maximum (FWHM) was equal to about 0.2°. The liquid sample, introduced in a Lindemann glass capillary (Ø = 0.7 mm), was mounted at the center of the goniometer circle G3000 and was rotated during the experiment around the vertical axis in order to ensure the proper averaging over the individual crystallites.

2. Raman spectroscopy

Liquid n-butanol was the input in a spherical pyrex cell (Ø = 5 mm), hermetically sealed. Raman spectra were collected on a XY Dilor spectrometer in back-scattering geometry, using the 514.5 nm light of a mixed Argon-Krypton Coherent laser. The same Oxford temperature device and the same thermal history of the sample described for X-ray diffraction experiments were used for the analysis of the OH stretching and the low-frequency regions in the different states of n-butanol.

In the low-frequency region, the Raman intensity in disordered states is related to the vibrational density of states [G(ω), VDOS] according to Refs. 17 and 18

$$I_{Raman}(\omega, T) = \frac{[n(\omega, T) + 1]}{\omega} C(\omega) G(\omega)$$

and $$\chi''(\omega) = \frac{C(\omega)}{\omega} G(\omega),$$

where n(ω) is the Bose-Einstein occupation factor, C(ω) is the light-vibration coupling coefficient, and $\chi''(\omega)$ was named Raman susceptibility. The frequency dependence of C(ω) has been widely investigated and much debated. Different descriptions have emerged from theoretical or experimental investigations leading to $C(\omega) = cst$,[18] $C(\omega) \propto \omega^2$,[19] and $C(\omega) \propto \omega$.[20,21] Also found was a universal linear behavior[22] $C(\omega) \propto (\omega/\omega_{BP} + B)$ near the boson peak (BP) maximum, with two groups of glasses corresponding to B = 0 and 0.5. In the case of ethanol, it was found[23] that B = 0.5, indicating that $\chi''(\omega)$ is not linearly proportional to G(ω). However, low-frequency dynamics in the fragile molecular glass former triphenyl phosphite[24] by coupled Raman and inelastic neutron scattering have shown that $\chi''(\omega)$ could be considered as representative of G(ω), with a spectrum resolution significantly higher than that obtained by inelastic neutron scattering.[24,25] Considering that Raman and neutron scattering investigations on molecular[24] and ionic[21] systems give similar descriptions for $\chi''(\omega)$ and G(ω), $\chi''(\omega)$ will be associated to the VDOS in the present study.

To obtain the $\chi''(\omega)$ spectrum plotted in Figure 1, the Raman intensity is first transformed into reduced intensity, plotted in the inset of Figure 1, using

$$I_r(\omega) = \frac{I_{Raman}}{[n(\omega) + 1]\omega}.$$

This relation promotes the quasielastic (QES) contribution usually fitted using a Lorentzian shape centered at

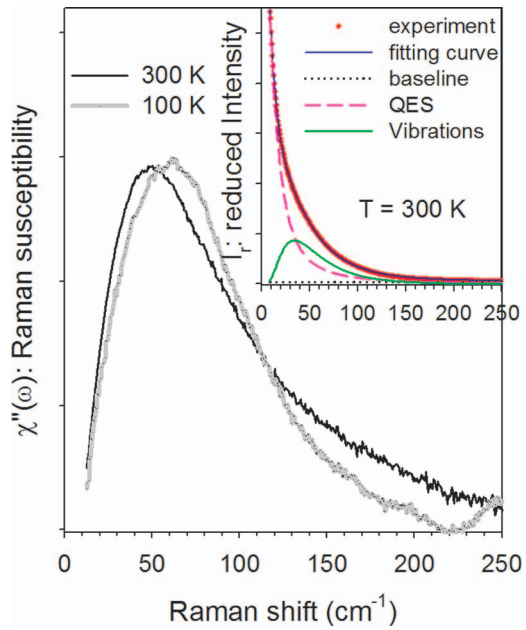

FIG. 1. Low-wavenumber Raman susceptibility of n-butanol at 100 K and 300 K. The fitting procedure of the reduced intensity at 300 K is plotted in the inset, with the determination of relaxational and vibrational contributions to the spectrum.

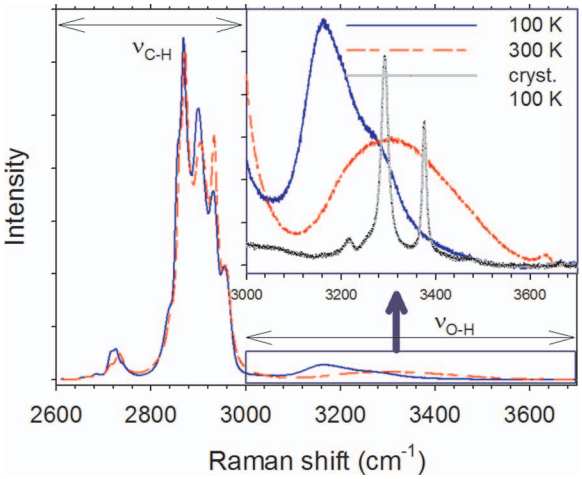

FIG. 2. High-wavenumber spectrum of n-butanol plotted at 100 K (glassy state) and 300 K (liquid state), composed of intramolecular CH (ν_{CH}) and OH (ν_{OH}) stretching bands. The inset corresponds to a zoom of the OH stretching region to clearly show the different band shapes at 100 and 300 K. The OH stretching spectrum of the crystal at 100 K was added in the inset, for comparing H-bonding in glassy, liquid, and crystalline states. Its intensity was divided by 5 for clarity.

$\omega = 0$. After subtracting the QES, the reduced intensity can be converted into Raman susceptibility $\chi''(\omega)$, as previously described.[10,24]

In the high-frequency region, Raman spectra were collected between 2610 and 3800 cm^{-1}. This region plotted in Figure 2 at T = 100 and 300 K, is dominated by the intramolecular CH stretching bands which are almost temperature independent. The intramolecular OH stretching spectrum covering the 3100–3700 cm^{-1} range was systematically normalized by the intensity of CH stretching bands, after subtraction of the baseline.

III. RESULTS

A. Analysis of amorphous n-butanol

1. Raman spectroscopy

a. Analysis of the low-wavenumber Raman spectrum in the 5–600 cm^{-1} wavenumber range. It is clearly observed in Figure 1 that the intensity maximum of $\chi''(\omega)$ shifts toward the high frequencies with temperature decreasing. The low-wavenumber vibrational excitations in the liquid state are generally interpreted as the wavenumber distribution of vibrations that molecules experience within the cage formed by their neighbors,[26] the so-called caging effect. The broadening of this distribution is related to the existence of disordered molecular environments corresponding to different cages. The $\chi''(\omega)$ spectra are fitted using a lognormal (LN) function, and the wavenumber ω_{LN} is plotted against the temperature in Figure 3. The temperature dependence of ω_{LN} is clearly nonlinear, reflecting a pronounced stiffening of the cages with temperature decreasing, drastically enhanced below T_m. The quantity $\chi''(\omega)/\omega^2$ is often used to highlight the existence of the BP in molecular systems, since the intensity of this contribution is usually low in fragile glass formers.[27] The BP is well recognized as reflecting the universal properties exhibited by glasses.[28] Among the different approaches proposed to understand the general behavior of glasses and the origin of BP, the phenomenological soft-potential model[29] is one of the most accepted.[30] However, the BP is often connected to the existence of heterogeneities and its band shape is fitted using a lognormal function, representative of a cluster size distribution,[28,31] the position of intensity maximum being inversely proportional to the mean size of clusters. $\chi''(\omega)/\omega^2$ spectra were calculated in the liquid state. A maximum of intensity in the spectra is detectable by decreasing the temperature from 183 K $\sim T_m$, down to the lower temperatures around 100 K, i.e., in the undercooled regime and the glassy state. The corresponding spectra are plotted in Figure 4 at several temperatures, and the wavenumber of the intensity maximum, determined by fitting procedures using a lognormal function, is plotted against T, below T_m, in the inset of Figure 4. The band shape of BP observed in Figure 4 can be considered as reflecting a size distribution of clusters corresponding to H-bonded molecular associations. The discontinuity at T_m of the position of the maximum intensity of BP can be interpreted as a decrease of the mean cluster size.

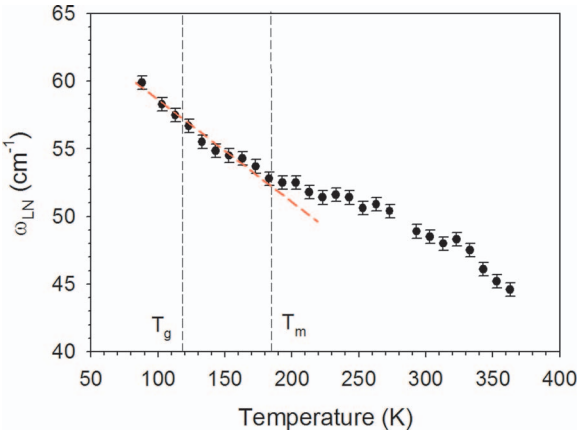

FIG. 3. Temperature dependence of the wavenumber corresponding to the maximum of Raman susceptibility. The dashed line is a guide for the eyes, to highlight the change in the ω(T)-behavior below T_m.

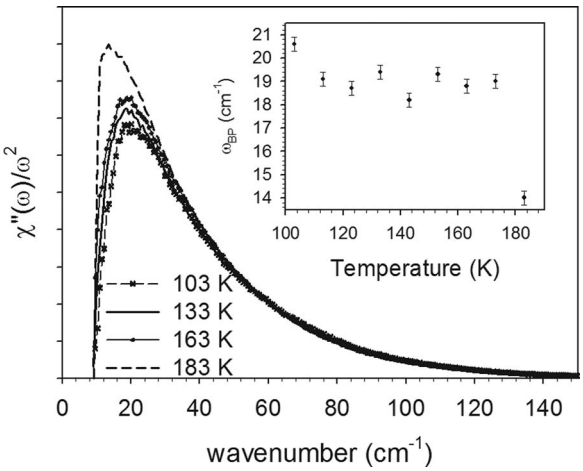

FIG. 4. Temperature dependence of the $\chi''(\omega)/\omega^2$-plot used to show the deviation of $\chi''(\omega)$ from the ω^2 behavior, and considered as the Boson peak. The temperature dependence of the wavenumber of the Boson peak, ω_{BP}(T), is shown in the inset.

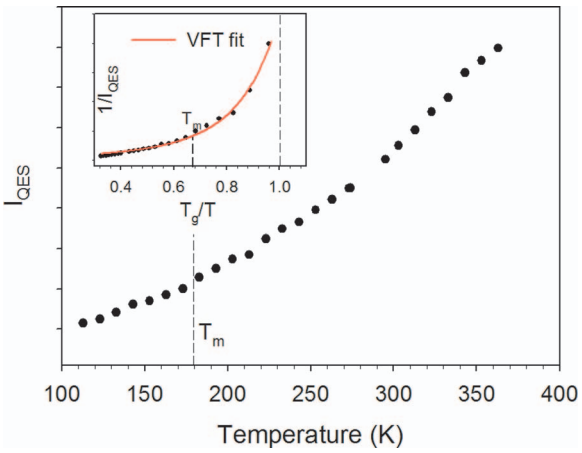

FIG. 5. Temperature dependence of the QES intensity, IQES. The temperature dependence of $1/I_{QES}$ (circles) is plotted against T_g/T, with the fitting curve (line) corresponding to the VFT function $\exp[A\times T_0/(T-T_0)]$ with $A = 6.7 \pm 0.1$ and $T_0 = 45$ K.

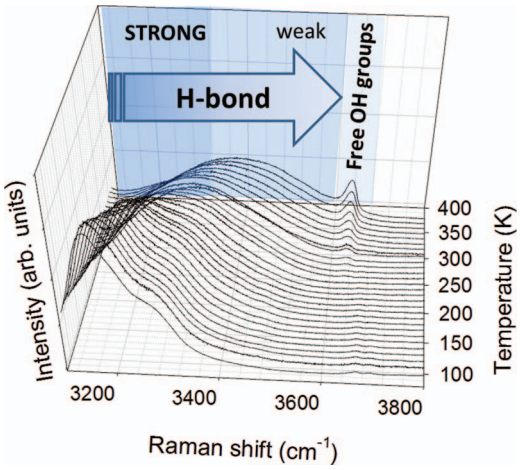

FIG. 6. Temperature dependence of the intramolecular OH stretching spectrum.

The procedure used to obtain $\chi''(\omega)$ spectra (Figure 1), also gives the Lorentzian band centered at zero wavenumber, reflecting the QES component. The temperature dependence of its intensity I_{QES} is similar to that of mean-squared relaxational displacement $1/\langle u^2\rangle_{rel}$,[27] usually determined from neutron scattering experiments. This $\langle u^2\rangle_{rel}$ term was considered as the driving force of the glass transition for fragile liquids,[27] and a linear relation $\langle u^2\rangle_{rel} \propto \log \eta$, where η is the viscosity, was experimentally determined in different glass-forming systems.[32] The intensity of the Lorentzian band is normalized using intramolecular bands in the 330–540 cm^{-1} region, as intensity reference, to obtain I_{QES} plotted against temperature in Figure 5. It is clearly observed that I_{QES} increases fast with temperature, as expected for the relaxational $\langle u^2\rangle_{rel}$ term in fragile glass-forming liquids.[27] This behavior is corroborated by the plot of $1/I_{QES}$ against T_g/T in the inset of Figure 5, which exhibits a non-Arrhenius character, well described by the Vogel-Fulcher-Tammann (VFT) function, $e^{A.T_0/(T-T_0)}$. The value $A = 6.7 \pm 0.1$ obtained from the fitting procedure corresponds to the curvature of the plot[33] distinctive of a fragile system. The value obtained for $T_0 = 45$ K is abnormally low, probably because of a lack of experimental data in the vicinity of T_g.

b. Analysis of the high frequency spectrum in the 2610–3800 cm^{-1} wavenumber range. Figure 2 shows that the 2610–3800 cm^{-1} region is dominated by the intense CH stretching bands. However, the most significant spectral modifications induced by temperature change, are observed in the OH stretching region. The temperature dependence of the Raman spectrum in the O–H stretching region is plotted in Figure 6 in the 100–363 K range, covering the glassy, the undercooled liquid, and the liquid states of n-butanol. In the low-temperature region, between 100 and 273 K, the spectrum is composed of a broad double hump lying on the 3100–3500 cm^{-1} wavenumber range. Above 273 K, the double hump structure transforms into a single and very broad band centered around 3400 cm^{-1} at 363 K, and a sharp band is merging around 3610 cm^{-1}, corresponding to OH stretching vibrations in non-associated molecules. The intensity increase of this band with temperature increasing reflects the dissociation of molecular associations above 270 K, leading to free OH groups. The spectrum of the OH stretching region can be well fitted using two Gaussian peaks in the 90–295 K temperature range. Above room temperature, both OH stretching bands are merging in a broad single band shape and cannot be deconvoluted with a satisfactory accuracy. The temperature dependences of the wavenumber and the integrated intensity of both OH stretching bands are plotted in Figures 7 and 8, respectively, in the 90 K–295 K. Figure 7 shows that both ω(T) variations are positive, and can be therefore considered as the signatures of two types of OH···O hydrogen bonds. The wavenumber of the stretching band gives information on the strength of the H-bond. The lower the wavenumber, the stronger is the H-bonding. The intensity of the OH stretching band is proportional to the number of H-bonds, and the intensity increase of these bands with temperature decreasing directly reflects the formation of H-bonds. The inspection of

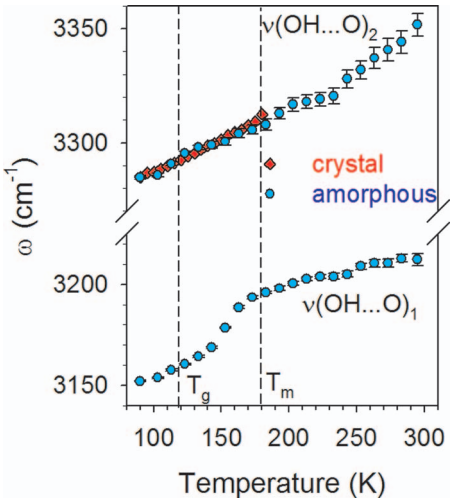

FIG. 7. Temperature dependence of the wavenumber of both OH stretching bands.

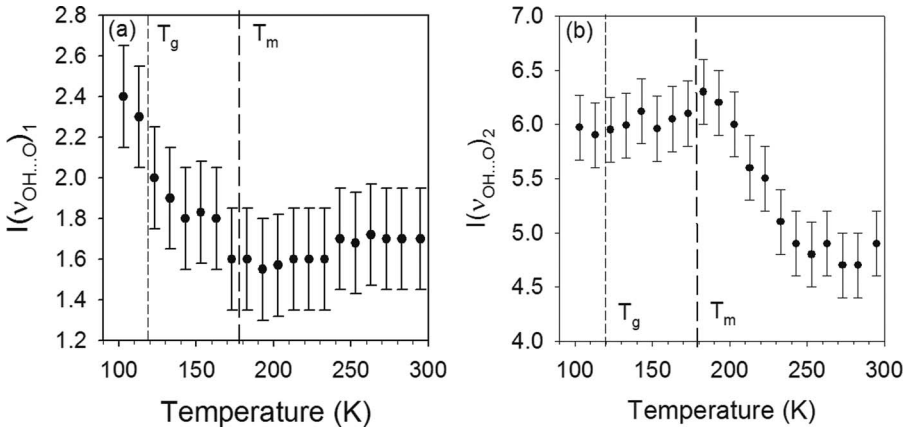

FIG. 8. Temperature dependence of the integrated intensity of (a) $\nu(OH\cdots O)_1$ and (b) $\nu(OH\cdots H)_2$ stretching bands.

Figures 6–8 indicates that the strong H-bonds $(OH\cdots H)_1$ corresponding to the low wavenumber band, are preferentially formed at low temperatures, in the undercooled regime. Below T_m, a change in the $\omega(T)$ curve is clearly observed, reflecting a strengthening of the $(OH\cdots H)_1$ H-bond specie. In contrast, the weak $(OH\cdots H)_2$ H-bond specie is predominant in the liquid state, above T_m.

2. X-ray diffraction

The intensity profile (I(Q)) of n-butanol was plotted in Figure 9 at four temperatures covering the investigated temperature range (90 K–400 K). I(Q) was normalized by the intensity maximum of the prepeak detected around 0.6 $Å^{-1}$. This prepeak, also called first sharp diffraction peak (FSDP), is observed in various alcohols[14,34] and more generally in H-bonded molecular liquids,[35] well below the main peak. It is considered as the signature of a structure, corresponding to some intermediate-range order (IRO) extending beyond the first shell of neighbors,[36] corresponding to hydrogen-bonded[35,37] molecular associations. Figure 9 clearly shows

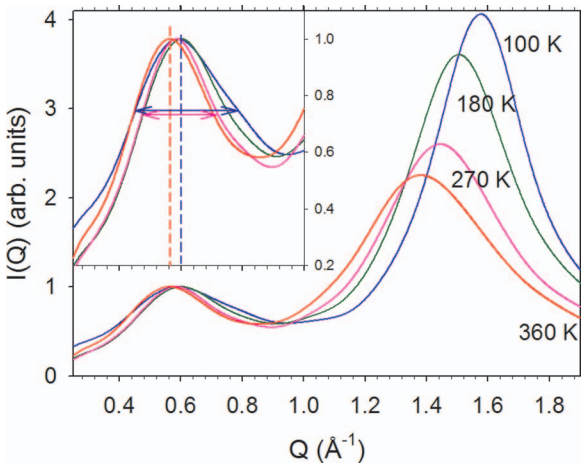

FIG. 9. Temperature dependence of the X-ray diffraction pattern of amorphous n-butanol in the 0.2–1.9 Q-range. The X-ray intensity was normalized by the intensity maximum of the FSDP. A zoom of the low-Q region is displayed in the inset to show the influence of temperature on the position and width of the FSDP.

that the position and the width are significantly temperature dependent, contrarily to other molecular materials.[35] The position and the width of the prepeak were determined by a fitting procedure of I(Q) in the 0.2–3.5 $Å^{-1}$ Q-range, using a Gaussian function for the prepeak and the main peak. The temperature dependences of both parameters are plotted in Figures 10(a) and 10(b). The position of the FSDP shifts from 0.53 $Å^{-1}$ up to 0.60 $Å^{-1}$, with temperature decreasing between 400 K and T_m, and remains nearly constant below T_m. The shift of the FSDP position, observed in Figure 10(a), reflects the decrease of the size of a structural organization from 12 Å near 400 K, down to 10.5 Å at T_m and below. Figure 10(b) shows an increase of the prepeak width with temperature decreasing below T_m, suggesting a decreasing correlation length[38] ($\ell_c = 2\pi/\Delta Q$) in the undercooled regime corresponding to a reduction of the coherence length from about 18.5 Å at T_m to 14 Å below T_g. It is worth noting that Figure 9 also indicates that the intensity of the prepeak increases with increasing temperature, as previously observed[11] and contrary to the intensity increase observed on cooling in other associated liquids,[35,39] interpreted as an increase of the mean number of clusters or their lifetime,[35] or as a change in the nature of the dominant form of clusters.[39]

B. Analysis of the devitrification process

1. Raman spectroscopy

The devitrification process was investigated by isothermal annealing of the undercooled liquid at $T_a = 120$ K, i.e., $T_g + 2$ K. We report here results obtained in previous studies.[10,16] The isothermal transformation of the undercooled liquid was observed to abort into a micro-crystallized state, called glacial state. The analysis of the glaciation gives the opportunity to obtain information on the early stages of the crystallization mechanism. The time dependence of the OH stretching spectrum during the isothermal transformation at $T_a = 120$ K has shown[10] that the low wavenumber component of the double hump disappears at the expense of two sharp bands, identified as the signatures of two types of O–H···O H-bonds in the stable crystal. The inset of Figure 2 shows that after cooling the crystal down to 100 K,

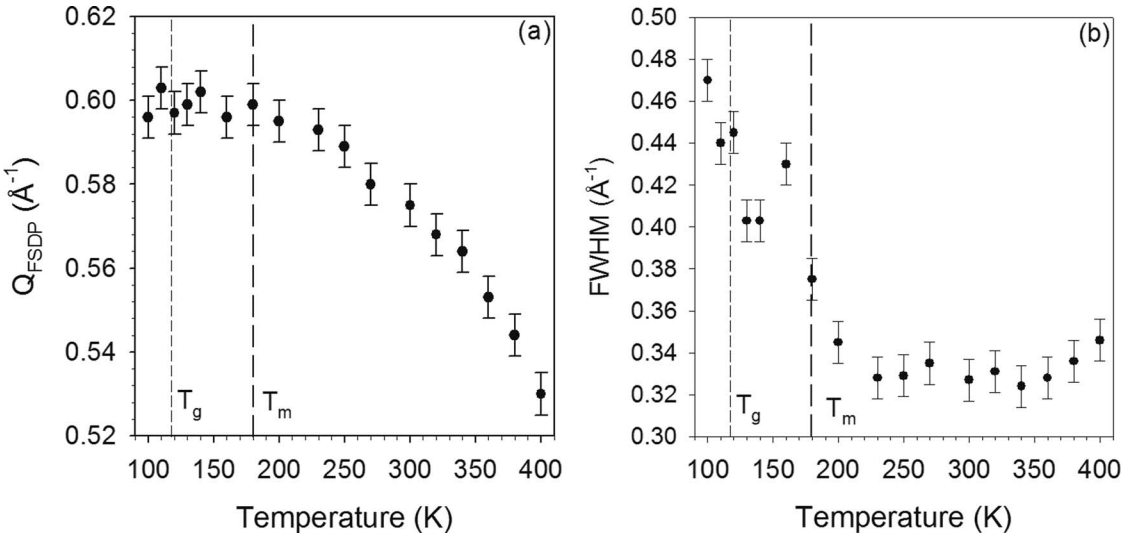

FIG. 10. Temperature dependence of the FSDP parameters; (a) position of intensity maximum: $Q_{FSDP}(T)$, (b) full width at half maximum: FWHM(T).

the most intense band, located around 3300 cm^{-1} corresponds to the high wavenumber component of the double hump in the OH stretching spectrum in the liquid state. The temperature dependence of this band analyzed in the crystal in a recent study[10] is plotted in Figure 7. Both temperature dependences in the crystal and the undercooled liquid state are superimposed below T_m. This similarity between the temperature dependences of the $\nu(OH\cdots O)_2$ wavenumber in the liquid and in the crystal, suggests that molecular associations via this type of H-bond are precursor of the long-range order. The less intense band [$\nu(OH\cdots O)_1$] emerging during the isothermal transformation and located around 3400 cm^{-1}, has no clear correspondence in the spectrum of the undercooled liquid, but is located under the broad $\nu(OH\cdots O)_2$ band of the liquid. Intriguingly, the strongest H-bond component disappears during the crystallization, and the long-range order in the crystal is characterized by weaker H-bonds than those predominant in the undercooled liquid state.

2. X-ray diffraction

The X-ray diffraction pattern was also collected during the isothermal transformation at 120 K, and the time dependence of the intensity profile is plotted in Figure 11. The most striking feature observed in Figure 11 is the coupled emergence of two peaks in the early stages of crystallization. A first broad peak grows at the expense of the prepeak, on the high-Q side of the prepeak, while a second sharp peak rapidly emerges on the high-Q side of the main peak. Both peaks are, respectively, located on the (001) and (012) Bragg peak positions of the crystal. It is worth noting that these crystalline signatures, growing during the isothermal transformation, were also observed on slow heating from the glassy state.[11] The emergence of these crystal features reflects the ordering of molecules which preferentially develops along the axis perpendicular to the long molecular axis with a high coherence length, and in a less extent along the [001]* direction. The growth of the sharp (012) peak observed in Figure 11 during the isothermal transformation of the undercooled liquid indicates that the early stages of crystallization correspond to the stacking of molecular layers perpendicular to the molecular axis, with a high coherence length. Simultaneously, the slow growth of the broadened (001) peak indicates the frustrated development of the preexisting molecular packing along the crystalline [001]* direction, corresponding to the IRO characterized by the FSDP. The structural organization in amorphous n-butanol extends over a size of 10–12 Å, slightly greater than the unit cell parameter (c ∼ 9 Å[16]). It is characterized by a distribution of OH···O distances corresponding to the broad $\nu(OH\cdots O)_2$ band, and probably to both OH···O bond species existing in the crystal. The frustration should be inherent to the pronounced contribution of strong H-bonds,

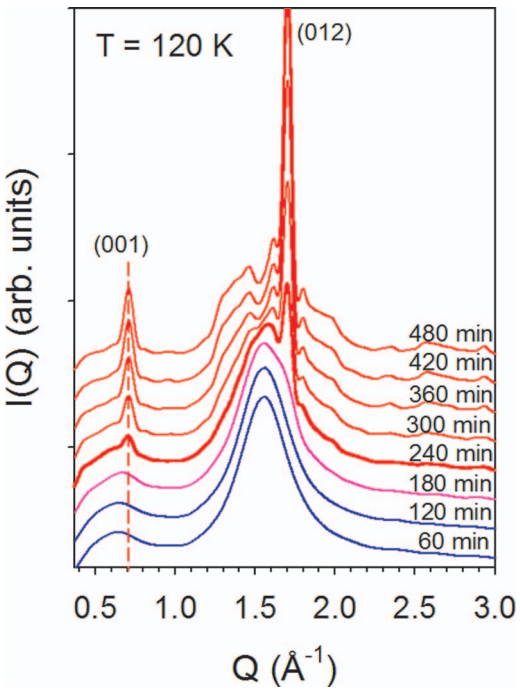

FIG. 11. Time dependence of the X-ray diffraction pattern during the isothermal transformation of the undercooled liquid into the glacial state at 120 K.

corresponding to the $\nu(OH\cdots O)_1$ band growing at the lower temperatures, and incompatible with the long-range order of the crystal.

IV. DISCUSSION

The detailed analysis of the dynamics of n-butanol, confronted with structural investigations in the different amorphous (liquid, undercooled liquid, glass) states gives information related to the undercooled liquid state and the inherent glass transition mechanism. The X-ray diffraction investigations have revealed the atypical temperature dependence of the FSDP in the amorphous states of n-butanol, compared to investigations performed in other associated molecular liquids,[35,39] in which the position and width of the FSDP were found temperature independent, and its intensity increases on cooling. In the H-bonded molecular liquids, the existence of this prepeak is usually related to some molecular organization at intermediate range, induced by H-bond associations.[14,34,35] In n-butanol, the presence of the FSDP in the X-ray diffraction pattern of the liquid state reflects molecular associations via $(OH\cdots H)_2$ H-bond specie above T_m. The temperature dependence of the FSDP position, plotted in Figure 10(a), can be interpreted as the increase of size of the molecular organization in the liquid state above T_m. A clear increase of the FSDP width is observed in Figures 9 and 10(b), below T_m, i.e., in the undercooled regime. This feature indicates a decrease of the coherence length with decreasing temperature. The intensity decrease of the prepeak on cooling, compared to the intensity of the main peak, is also an atypical temperature behavior, previously interpreted as reflecting a change in the shape of reflection volumes, corresponding to the collection of molecules which produce this FSDP.[11] These original observations can be related to the formation of the strong $(OH\cdots H)_1$ H-bond below T_m, clearly evidenced in Figures 6 and 8(a). The atypical temperature behavior of the prepeak (position, width, and intensity) can be considered as the signature of a gradual change in the dominant specie of H-bonded molecular associations. This change is consistent with the interpretation of the temperature behavior of the prepeak intensity in terms of change in the shape of clusters proposed by Shmyt'ko *et al.*[11] The strong H-bond specie becomes gradually pronounced on cooling at low temperature (below T_m) but is not compatible with the development of the long-range order, since Figure 2 clearly shows that the corresponding OH stretching band $[\nu(OH\cdots O)_1]$ disappears during crystallization and is not detected in the crystal. It is noticeable that below T_m, a change in the $\omega_{LN}(T)$ curve is observed in Figure 3. This effect indicates a hardening of the collective vibrations, probably associated with the enhancement of the VDOS at the low-wavenumbers, detected via the plot of $\chi''(\omega)/\omega^2$ in Figure 4. A more rigid molecular cage is expected with temperature decreasing, and can explain an increase of ω_{LN}. The formation of strong H-bonding can also be responsible for a stiffening of the environment experienced n-butanol molecules, leading to an enhanced increase of ω_{LN} by temperature decreasing below T_m. It could also be responsible for a decrease of cluster size, detected via the discontinuity of the BP position at T_m. These features show clear correlations between the formation of strong H-bond specie, the collective vibrations, and structural heterogeneities in the undercooled liquid state. The development of an additional $(OH\cdots H)_1$ type of molecular associations coexisting with the $(OH\cdots H)_2$ H-bond network, corresponding to the predominant molecular associations in the liquid state and precursor of the long-range order, can explain the decrease of the coherence length of the intermediate-range order. In this context, the undercooled regime could be interpreted as resulting from the competition between the development of a preferred local organization at low temperature, characterized by molecular associations via strong $(OH\cdots H)_1$ H-bonds and the extension of the intermediate-range order characterized by molecular associations via softer $(OH\cdots H)_2$ H-bonds. Given the strengthening of H-bonding corresponding to the $\nu(OH\cdots O)_1$-band below T_m (Figure 7), this competition can also explain the abortive crystallization into the glacial state at temperatures slightly above T_g, as suggested in a previous study.[10]

V. CONCLUSION

We have performed complementary Raman and X-ray diffraction experiments in the amorphous (liquid, undercooled liquid, and glassy) states of n-butanol. Raman investigations performed both in the low-wavenumber range and in the OH stretching region give information on fast mean-squared displacement, collective vibrations, and molecular associations via H-bonds. X-ray diffraction was used to probe local structural organizations via the analysis of the prepeak. Clear correlations were pointed out between the temperature dependence of the collective vibrational excitations and that of the prepeak width, in relation with molecular associations via H-bonding. The development of molecular associations via strong H-bond below T_m, was found as being a frustration for crystallization, and the associated dynamical and structural properties as signatures of the undercooled liquid regime of n-butanol.

[1] C. A. Angell, K. Ngai, G. B. McKenna, P. F. McMillan, and S. W. Martin, J. Appl. Phys. **88**, 3113 (2000).
[2] A. Ha, I. Cohen, X. Zhao, M. Lee, and D. Kivelson, J. Phys. Chem. **100**, 1 (1996).
[3] I. Cohen, A. Ha, X. Zhao, M. Lee, T. Fisher, M. J. Strouse, and D. Kivelson, J. Phys. Chem. **100**, 8518 (1996).
[4] B. V. Bol'shakov and A. G. Dzhonson, J. Non-Cryst. Solids **351**(5), 444 (2005).
[5] R. Kurita and H. Tanaka, J. Phys.: Condens. Matter **17**(27), L293 (2005).
[6] D. Kivelson, S. A. Kivelson, X. Zhao, Z. Nussinov, and G. Tarjus, Physica A **219**(1–2), 27 (1995).
[7] A. Hédoux, Y. Guinet, P. Derollez, O. Hernandez, R. Lefort, and M. Descamps, Phys. Chem. Chem. Phys. **6**(12), 3192 (2004).
[8] A. Hédoux, Y. Guinet, P. Derollez, O. Hernandez, L. Paccou, and M. Descamps, J. Non-Cryst. Solids **352**, 4994 (2006); A. Hedoux, Y. Guinet, and M. Descamps, Phys. Rev. B **58**(1), 31 (1998).
[9] P. Derollez, O. Hernandez, A. Hédoux, Y. Guinet, O. Masson, J. Lefebvre, and M. Descamps, J. Mol. Struct. **694**, 131 (2004); O. Hernandez, A. Hédoux, J. Lefebvre, Y. Guinet, M. Descamps, R. Papoular, and O. Masson, J. Appl. Crystallogr. **35**, 212 (2002).
[10] A. Wypych, Y. Guinet, and A. Hédoux, Phys. Rev. B **76**, 144202 (2007).
[11] I. M. Shmyt'ko, R. J. Jimenez-Rioboo, M. Hassaine, and M. A. Ramos, J. Phys.: Condens. Matter **22**, 195102 (2010).
[12] M. Hassaine, R. J. Jimenez-Rioboo, I. V. Sharapova, O. A. Korolyuk, A. I. Krivchikov, and M. A. Ramos, J. Chem. Phys. **131**, 174508 (2009).

[13]P. Derollez, A. Hédoux, Y. Guinet, J. Lefebvre, M. Descamps, and O. Hernandez, Z. Kristallogr. Suppl. **23**, 557 (2006).
[14]K. S. Vahvaselka, R. Serimaa, and M. Torkkeli, J. Appl. Crystallogr. **28**, 189 (1995).
[15]G. Adam and J. H. Gibbs, J. Chem. Phys. **43**, 139 (1965).
[16]P. Derollez, A. Hédoux, Y. Guinet, F. Danede, and L. Paccou, Acta Crystallogr., Sect. B: Struct. Sci. **69**, 195 (2013).
[17]F. L. Galeener and P. N. Sen, Phys. Rev. B **17**(4), 1928 (1978).
[18]R. Shuker and R. Gammon, Phys. Rev. Lett. **25**(4), 222 (1970).
[19]A. J. Martin and W. Brenig, Phys. Status Solidi B **64**, 163 (1974).
[20]A. P. Sokolov, A. Kisliuk, D. Quitmann, and E. Duval, Phys. Rev. B **48**, 7692 (1993).
[21]A. Fontana, F. Rocca, M. P. Fontana, B. Rossi, and A. J. Dianoux, Phys. Rev. B **41**(6), 3778 (1990).
[22]N. V. Surovtsev and A. P. Sokolov, Phys. Rev. B **66**, 54205 (2002).
[23]N. V. Surovtsev, S. V. Adichtchev, E. Rossler, and M. A. Ramos, J. Phys.: Condens. Matter **16**, 223 (2004).
[24]A. Hédoux, P. Derollez, Y. Guinet, A. J. Dianoux, and M. Descamps, Phys. Rev. B **63**, 144202 (2001).
[25]A. Hédoux, Y. Guinet, and M. Descamps, Int. J. Pharm. **417**, 17 (2011).
[26]J. A. Padro and J. Marti, J. Chem. Phys. **118**(1), 452 (2003).
[27]A. P. Sokolov, E. Rossler, A. Kisliuk, and D. Quitmann, Phys. Rev. Lett. **71**, 2062 (1993).
[28]V. K. Malinovski and A. P. Sokolov, Solid State Commun. **57**(9), 757 (1986).
[29]V. G. Karpov, M. I. Klinger, and F. N. Ignat'ev, Zh. Eksp. Teor. Fiz. **84**, 760 (1983); Sov. Phys. JETP **57**, 439 (1983).
[30]M. A. Ramos, C. Talon, and S. Vieira, J. Non-Cryst. Solids **307–310**, 80 (2002).
[31] E. Duval, A. Boukenter, and T. Achibat, J. Phys.: Condens. Matter **2**(51), 10227 (1990); I. Pocsik and M. Koos, Solid State Commun. **74**, 1253 (1990).
[32]U. Buchenau and R. Zorn, Europhys. Lett. **18**, 523 (1992); M. C. C. Ribeiro, J. Chem. Phys. **133**, 024503 (2010).
[33]C. A. Angell, Chem. Rev. **102**(8), 2627 (2002).
[34]A. K. Karmakar, P. S. R. Krishna, and R. N. Joarder, Phys. Lett. A **253**, 207 (1999).
[35]D. Morineau and C. Alba-Simionesco, J. Chem. Phys. **109**(19), 8494 (1998).
[36]S. R. Elliott, Nature (London) **354**(6353), 445 (1991); J. Phys.: Condens. Matter **4**(38), 7661 (1992).
[37]A. H. Narten and A. Habenschuss, J. Chem. Phys. **80**, 3387 (1984).
[38]R. Fayos, F. J. Bermejo, J. Dawidowski, H. E. Fischer, and M. A. Gonzalez, Phys. Rev. Lett. **77**(18), 3823 (1996).
[39]A. Sahoo, S. Sarkar, P. S. Krishna, and R. N. Joarder, Pramana, J. Phys. **63**, 183 (2004).